

Supporting Information

Indoor partitioning and potential thirdhand exposure to carbonyl flavoring agents added in e-cigarette and hookah tobacco

1

Shuang Wu,[†] Erica Kim,[†] Dilini Vethanayagam,[‡] and Ran Zhao^{*,†}

[†]*Department of Chemistry, University of Alberta, Edmonton, Alberta, T6G 2G2, Canada*

[‡]*Department of Medicine, University of Alberta, Edmonton, Alberta, T6G 2G2, Canada*

E-mail: rz@ualberta.ca

2 **Section S1.** Structures of flavoring compounds

3 **Section S2.** Plots of $\ln(C_t/C_0)$ versus time for all target flavorings

4 **Section S3.** Choice of setups with different purging bubble size

5 **Section S4.** Log K_{wa} and log K_{oa} values used in 2D partitioning plots

6 **Section S5.** Summary of the measured effective Henry's law constant ($H_{s,eff}^{cp}$)

7 **Section S6.** Syringe pump-GC setup

8 **Section S7.** Summary of the hydration equilibrium constant (K_{hyd}) and the intrinsic
9 Henry's law constant (H_s^{cp})

10 **Section S8.** Comparison between the effective Henry's law constant ($H_{s,eff}^{cp}$) and the
11 intrinsic Henry's law constant (H_s^{cp})

12 **Section S1.** Structures of flavoring compounds

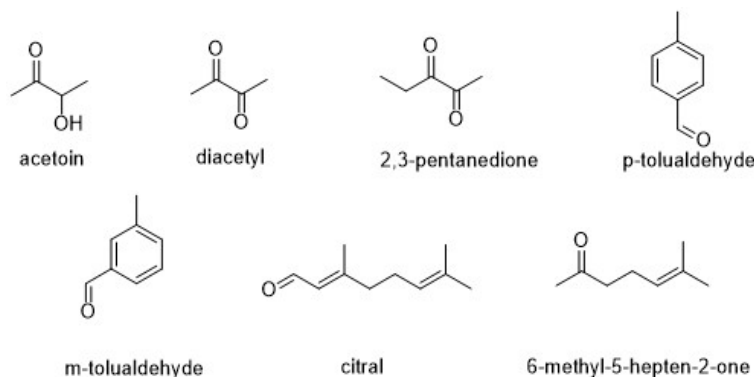


Figure S1: Structures of the flavoring compounds.

13 **Section S2.** Plots of $\ln(C_t/C_0)$ versus time for all target flavorings

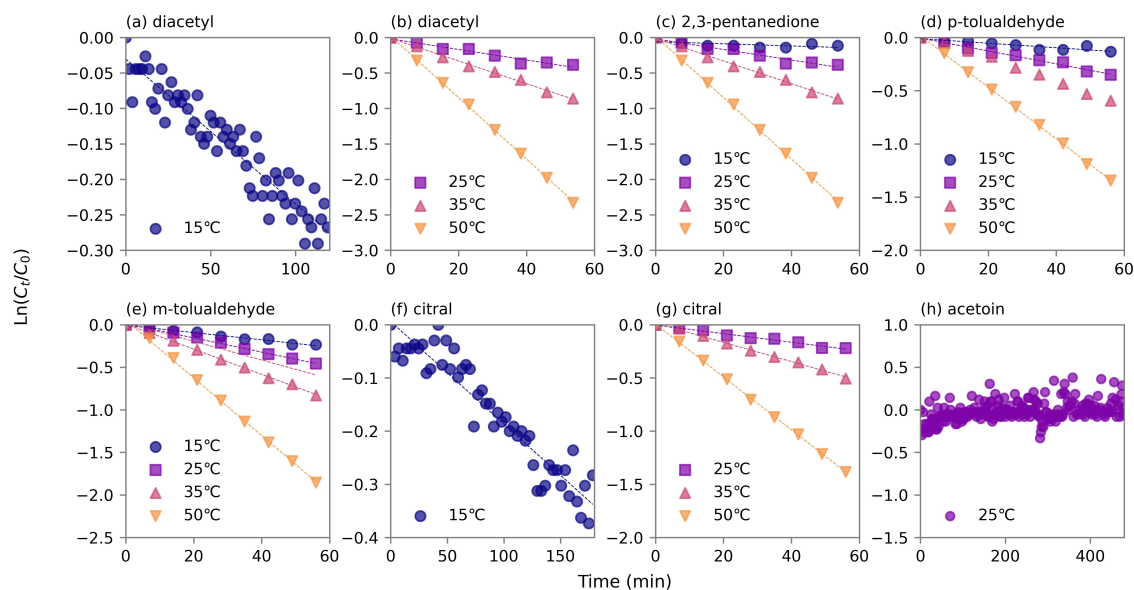


Figure S2: Plots of $\ln(C_t/C_0)$ versus time at 15, 25, 35 and 50 °C for all target flavorings. (a) Diacetyl at 15 °C; (b) Diacetyl at 25, 35 and 50 °C; (c) 2,3-Pentanedione; (d) p-Tolualdehyde; (e) m-Tolualdehyde; (f) Citral at 15 °C; (g) Citral at 25, 35 and 50 °C; (h) Acetoin at 25 °C.

14 **Section S3.** Choice of setups with different purging bubble sizes

15 Previous studies have demonstrated that the adsorption of the target molecule to the bubble
 16 surface can cause bias in the IGS method, and 0.001 m has been suggested as an interface-air
 17 adsorption coefficient (K_{ia}) threshold when applying the small bubbles.¹ Briefly, K_{ia} , in the
 18 unit of m, is expressed as the partitioning coefficient between the water-air interface (on the
 19 bubble surface) and the gas phase (inside the bubble).² Following this conclusion, another
 20 paper recommended large bubbles (diameter around 5.5 mm) be applied for chemicals with
 21 large K_{ia} (below 0.02 m).³

Table S1: K_{ia} values, difference percentage of the measured $H_{s,eff}^{cp}$ between two setups and accordingly setup choice for target flavorings.

	Log K_{ia} at 15 °C ⁴	$H_{s,eff}^{cp}$ difference at 25 °C (%)	Bubble size ^b
diacetyl ^a	-3.89	n.d.	small
2,3-pentanedione	n.a.	1.14%	small
p-tolualdehyde	-3.41	n.d.	small
m-tolualdehyde	-3.44	n.d.	small
6-methyl-5-hepten-2-one	n.a.	7.79%	small
citral	-2.31	n.d.	large

^aTesting compound. ^bSmall bubbles are ~3 mm in diameter with flow rate 100 sccm, large bubbles are ~6 mm in diameter with flow rate 200 sccm. n.d.: Not detected due to the known K_{ia} value. n.a.: Not available.

22 Two bubbler-column setups have been used according to the K_{ia} values of the target
 23 compounds, see Table S1. One setup produces small bubbles (diameter around 3 mm) with
 24 a flow rate of 100 sccm for diacetyl, p-tolualdehyde and m-tolualdehyde, which have small
 25 K_{ia} values. Another one with a single-perforation on the glass head, produces large bubbles
 26 (diameter around 6 mm) for citral with large K_{ia} values. The K_{ia} values were predicted
 27 by an online UFZ-LSER database based on a poly-parameter linear free-energy relationship
 28 (pp-LFERs).^{2,4} Please note that there are no available model-predicted K_{ia} values for 2,3-
 29 pentanedione and 6-methyl-5-hepten-2-one, we decided to use small bubbles because of the
 30 differences between the results obtained by the two setups were less than 10% at 25 °C.

31 **Section S4.** Log K_{wa} and log K_{oa} values used in 2D partitioning plots

Table S2: Log K_{wa} and log K_{oa} values used in 2D partitioning plots for target flavourings.

	15 °C		25 °C		35 °C		50 °C	
	log K_{wa}	log K_{oa}						
diacetyl ^a	3.48	3.90	3.13	3.55	2.81	3.31	2.40	3.02
2,3-pentanedione	3.37	4.18	2.94	3.85	2.59	3.67	2.15	3.34
p-tolualdehyde	3.40	5.63	3.00	5.25	2.71	5.05	2.35	4.71
m-tolualdehyde	3.16	5.57	2.86	5.20	2.62	5.01	2.25	4.66
6-methyl-5-hepten-2-one	2.77	5.38	2.44	4.99	2.20	4.82	1.79	4.50
citral	3.18	6.12	2.87	5.69	2.55	5.52	2.14	5.17

^aTesting compound.

Table S3: Log K_{wa} and log K_{oa} values used in 2D partitioning plots for other frequently added flavourings in e-cigarettes at 25 °C.

	log K_{wa} ^a	log K_{oa} ^b	K_{hyd} ^b
vanillin	7.07	7.5	0.002
ethyl butyrate	1.77	3.64	0.018
ethyl acetate	2.27	2.95	0.033
maltol	5.85 ^b	7.49	n.a.
ethyl vanillin	7.47	8.05	0.002
cis-3-hexenol	3.55 ^b	5.46	n.a.
isoamyl acetate	2.73	4.11	0.027
linalool	2.94	6.50	n.a.
benzyl alcohol	4.90	6.04	n.a.
benzaldehyde	1.94	4.68	0.011

^aThe average of previous published data summarized by Sander unless otherwise noted.⁵ ^bPredicted data from SPARC.⁶ n.a.: Not available.

32 **Section S5.** Summary of the measured effective Henry’s law constant ($H_{s,\text{eff}}^{\text{cp}}$)

Table S4: Summary of the measured $H_{s,\text{eff}}^{\text{cp}}$ for target flavorings at different temperatures with two bubbler setups.

	Temperature(°C)	$H_{s,\text{eff}}^{\text{cp}}$ (mol·m ⁻³ ·Pa ⁻¹)	Bubble size ^b
diacetyl ^a	15	1.27 ± 0.05	small
	25	(5.50 ± 0.18) × 10 ⁻¹	small
	35	(2.52 ± 0.07) × 10 ⁻¹	small
	50	(9.44 ± 0.25) × 10 ⁻²	small
2,3-pentanedione	15	(9.86 ± 1.06) × 10 ⁻¹	small
	25	(3.50 ± 0.33) × 10 ⁻¹	small
	25	(3.54 ± 0.46) × 10 ⁻¹	large
	35	(1.51 ± 0.03) × 10 ⁻¹	small
	50	(5.28 ± 0.10) × 10 ⁻²	small
p-tolualdehyde	15	1.06 ± 0.05	small
	25	(4.22 ± 0.13) × 10 ⁻¹	small
	35	(2.16 ± 0.07) × 10 ⁻¹	small
	50	(9.24 ± 0.10) × 10 ⁻²	small
m-tolualdehyde	15	(6.00 ± 0.37) × 10 ⁻¹	small
	25	(2.92 ± 0.02) × 10 ⁻¹	small
	35	(1.62 ± 0.02) × 10 ⁻¹	small
	50	(6.61 ± 0.08) × 10 ⁻²	small
6-methyl-5-hepten-2-one	15	(2.44 ± 0.10) × 10 ⁻¹	small
	25	(1.11 ± 0.04) × 10 ⁻¹	small
	25	(1.20 ± 0.06) × 10 ⁻¹	large
	35	(6.24 ± 0.07) × 10 ⁻²	small
	50	(2.30 ± 0.02) × 10 ⁻²	small
citral	15	(6.33 ± 0.91) × 10 ⁻¹	large
	25	(2.99 ± 0.29) × 10 ⁻¹	large
	35	(1.37 ± 0.11) × 10 ⁻¹	large
	50	(5.15 ± 0.51) × 10 ⁻²	large

^aTesting compound. ^bSmall bubbles are ~3 mm in diameter with flow rate 100 sccm, large bubbles are ~6 mm in diameter with flow rate 200 sccm.

33 **Section S6.** Syringe pump-GC setup for acetoin

34 Given that our IGS setup was unable to determine the $H_{s,\text{eff}}^{\text{cp}}$ of acetoin, we have attempted
 35 to determine it by taking the ratio between its aqueous- and gas-phase concentrations at
 36 equilibrium, according to eq 1 introduced in the main article:

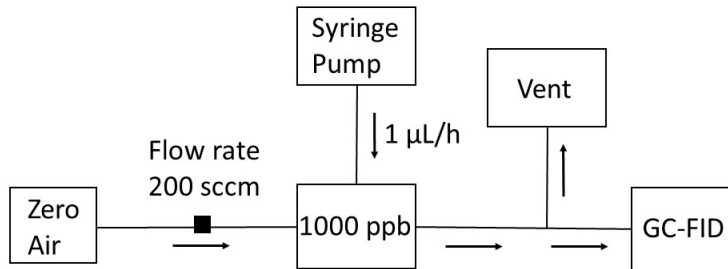


Figure S3: Schematic of syringe pump-GC setup.

$$K_{wa} = c_l/c_g \quad (\text{S1})$$

37 where c_l is the known concentration of acetoin in the aqueous solution inside the bubbler.
 38 c_g is the gas-phase concentration of acetoin at equilibrium. To determine c_g , we have utilized
 39 a syringe pump-GC setup (Figure S3) to calibrate the GC-FID signal of acetoin. Briefly, a
 40 known amount of acetoin was diluted in methanol and placed in a 100 μL gas-tight syringe
 41 (Hamilton, USA). The syringe pump injected the solution into the glass container at a rate
 42 of 1 $\mu\text{L}/\text{h}$, and the liquid was assumed to be fully volatilized with a stream of zero air (200
 43 sccm) flowing through the container. The sample was injected into GC-FID via the gas-
 44 sampling valve automatically, and the acetoin signal was monitored over eight hours. As
 45 a result, a signal (0.075 $\text{pA}\cdot\text{min}$) was obtained with a 1000 ppb gas concentration in the
 46 glass container, which was translated into a calibration factor of our GC-FID for acetoin. In
 47 the IGS setup, the 0.02 g/L acetoin solution gave a stable signal (0.038 $\text{pA}\cdot\text{min}$) after eight
 48 hours in both bubblers with different bubble sizes. Therefore, the estimated $H_{s,\text{eff}}^{\text{cp}}$ for acetoin
 49 at 25 $^\circ\text{C}$ is 4.0 $\text{mol}\cdot\text{m}^{-3}\cdot\text{Pa}^{-1}$. Considering potential wall loss of acetoin (glass and tube) and
 50 the fact that the chemical may not be fully volatilized, the value of 4.0 $\text{mol}\cdot\text{m}^{-3}\cdot\text{Pa}^{-1}$ should
 51 be considered an upper limit.

52 **Section S7.** Summary of the hydration equilibrium constant (K_{hyd}) and the intrinsic
 53 Henry's law constant (H_{s}^{CP})

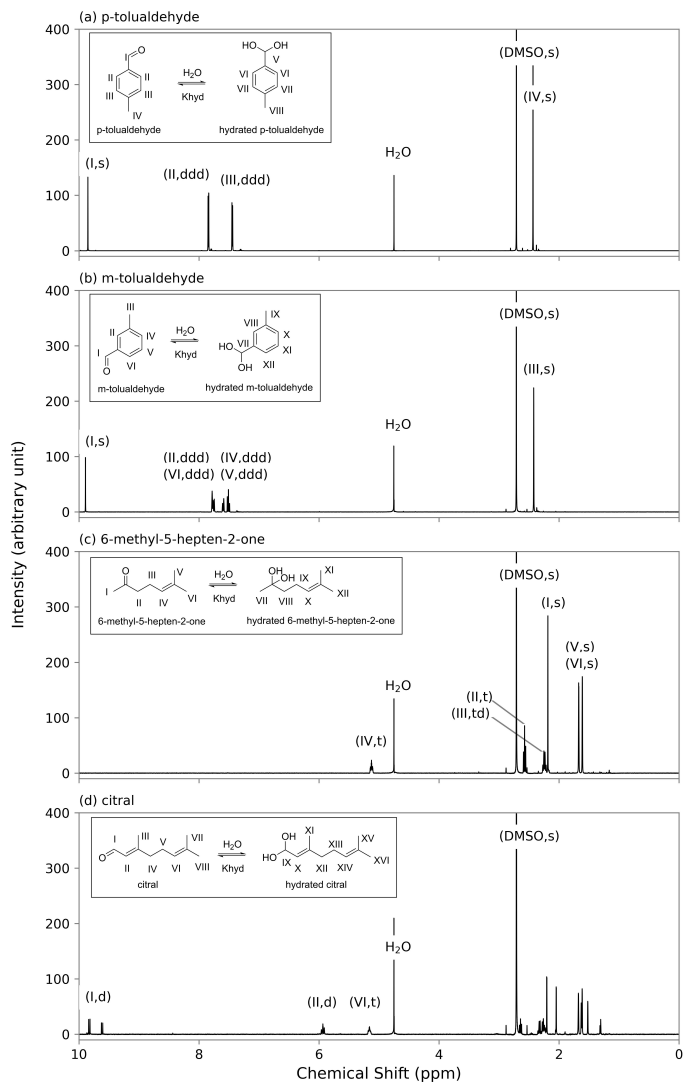


Figure S4: ^1H NMR spectra for the flavoring agents diluted in D_2O with DMSO as an internal standard at 25°C . (a) p-Tolualdehyde; (b) m-Tolualdehyde; (c) 6-Methyl-5-hepten-2-one; (d) Citral. The identity of the peak (the numbers match those in the chemical structures) and splitting pattern are shown in the brackets. Schematics of the hydration processes are included.

54 In order to determine K_{hyd} , quantifications for one peak from carbonyl and another
 55 from hydrated carbonyl are needed according to eq 6. Figure S4 presents the spectra for
 56 p-tolualdehyde, m-tolualdehyde, 6-methyl-5-hepten-2-one and citral, with the peak assign-

57 ments displayed in brackets, including chemical shift and the splitting pattern. The H₂O
58 singlet peak shows up at around 4.75 ppm, while the DMSO singlet peak is observed at
59 around 2.71 ppm. However, hydrated peaks have not been identified in their spectra. In
60 Figure S4(a), the peaks for non-hydrated p-tolualdehyde are shown in the spectrum. The
61 singlet peak V for hydrated p-tolualdehyde didn't appear at around 6.11 ppm as predicted;
62 other peaks such as (VI, ddd), (VII, ddd) and (VIII, s), that are supposed to show up at
63 around 7.26 ppm, 7.25 ppm and 2.23 ppm, respectively, might be overlapping with peak III
64 and IV. For the hydrated m-tolualdehyde in Figure S4(b), the singlet peak labeled as VII is
65 predicted to be at approximately 6.13 ppm, and likewise, a singlet peak IX to be around 2.29
66 ppm; however, there were no peaks observed at these chemical shifts. The other four protons
67 (VIII, X, XI, and XII) on the benzene ring with the ddd multiplicity are predicted to ap-
68 pear between 7 to 7.4ppm. These peaks were not observed either. Though, they might be
69 overlapping with m-tolualdehyde peaks. In Figure S4(c), the hydrated 6-methyl-5-hepten-
70 2-one peaks labeled as VII and IX are predicted to be at around 1.21ppm and 2.04 ppm
71 with multiplicity s and td, respectively. Based on our observation, there is no peak identified
72 under the influence of noise. The hydrated peaks triplet VIII and singlet peaks IX and XI
73 have chemical shifts between 1.56 to 1.57ppm, which are likely overlapping with peaks V
74 and VI due to the tiny signal. As a result of the geometric stereoisomersthere for citral,
75 there are two groups of doublet peaks from the peak I at 9.81 ppm and 9.78 ppm in Figure
76 S4(d). Besides the labeled citral peaks, other citral peaks are challenging to identify due to
77 the peak overlapping, especially between 1.5 to 2.5 ppm and the impurity of the citral (95%
78 purity, a mixture of cis- and trans-citral). Such as (III, s), (IV, t), (V, td), (VII, s) and
79 (VIII, s). Similarly, it is hard to identify hydrated peaks (XI, d), (XII, t), (XIII, td), (XV,
80 s), and (XVI, s) that show up between 1.5 to 2.5 ppm. By contrast, hydrated citral peaks,
81 including doublet IX, doublet X and triplet XIV are predicted to be at 5.12 to 5.28 ppm,
82 but there is no peak observed.

Table S5: Comparison of the measured K_{hyd} values with the predicted values for target flavorings.

	K_{hyd} at 25°C	
	NMR	SPARC ⁶
diacetyl ^a	2.52 ± 0.10	2.047
acetoin	$(1.92 \pm 0.10) \times 10^{-2}$	0.099
2,3-pentanedione	1.88 ± 0.09	1.164
2,3-pentanedione- K_{hyd_1}	$(9.20 \pm 0.25) \times 10^{-1}$	0.543
2,3-pentanedione- K_{hyd_2}	$(9.60 \pm 0.83) \times 10^{-1}$	0.621
p-tolualdehyde	n.d.	0.004
m-tolualdehyde	n.d.	0.007
6-methyl-5-hepten-2-one	n.d.	0.014
citral	n.d.	0.003

^aTesting compound. n.d.: Not detected due to the absence of the hydrated product peak.

Table S6: Summary of the K_{hyd} and H_{s}^{cp} at different temperatures for diacetyl, acetoin and 2,3-pentanedione.

	Temperature(°C)	K_{hyd}	$H_{\text{s}}^{\text{cp}}(\text{mol}\cdot\text{m}^{-3}\cdot\text{Pa}^{-1})$
diacetyl ^a	15	4.29 ± 0.14	$(2.40 \pm 0.13) \times 10^{-1}$
	25	2.50 ± 0.10	$(1.56 \pm 0.08) \times 10^{-1}$
	35	2.13 ± 0.10	$(8.05 \pm 0.45) \times 10^{-2}$
	50	1.39 ± 0.02	$(3.95 \pm 0.12) \times 10^{-2}$
acetoin	15	$(2.97 \pm 0.05) \times 10^{-2}$	n.d.
	25	$(1.92 \pm 0.10) \times 10^{-2}$	n.d.
	35	$(1.58 \pm 0.06) \times 10^{-2}$	n.d.
	50	$(1.16 \pm 0.02) \times 10^{-2}$	n.d.
2,3-pentanedione	15	2.52 ± 0.10	$(2.80 \pm 0.32) \times 10^{-1}$
	25	1.88 ± 0.09	$(1.22 \pm 0.13) \times 10^{-1}$
	35	1.40 ± 0.02	$(6.28 \pm 0.16) \times 10^{-2}$
	50	$(9.69 \pm 0.25) \times 10^{-1}$	$(2.68 \pm 0.09) \times 10^{-2}$
2,3-pentanedione- K_{hyd_1}	15	1.29 ± 0.07	n.a.
	25	$(9.20 \pm 0.25) \times 10^{-1}$	n.a.
	35	$(7.13 \pm 0.08) \times 10^{-1}$	n.a.
	50	$(4.78 \pm 0.09) \times 10^{-1}$	n.a.
2,3-pentanedione- K_{hyd_2}	15	1.23 ± 0.07	n.a.
	25	$(9.60 \pm 0.83) \times 10^{-1}$	n.a.
	35	$(6.92 \pm 0.18) \times 10^{-1}$	n.a.
	50	$(4.91 \pm 0.23) \times 10^{-1}$	n.a.

^aTesting compound. n.d.: Not detected due to the absence of signal decay in $H_{\text{s,eff}}^{\text{cp}}$ measurement. n.a.: Not available.

83 **Section S8.** Comparison between the effective Henry’s law constant ($H_{s,\text{eff}}^{\text{cp}}$) and the intrinsic
 84 Henry’s law constant (H_s^{cp})

Table S7: K_{hyd} , $H_{s,\text{eff}}^{\text{cp}}$, H_s^{cp} , $\log K_{\text{wa,eff}}$ and $\log K_{\text{wa}}$ values at 25°C for target flavorings and representative carbonyls.

	K_{hyd}^b	$H_{s,\text{eff}}^{\text{cp}b}$	$H_s^{\text{cp}c}$	$\log K_{\text{wa}}^d$	$\log K_{\text{wa,eff}}^d$
diacetyl ^a	2.52	0.55	0.16	2.59	3.13
2,3-pentanedione	1.88	0.35	0.12	2.48	2.94
acetoin	0.02	0.57 ^e	0.56	3.14	3.15
p-tolualdehyde	n.d.	0.42	0.42	3.02	3.02
m-tolualdehyde	n.d.	0.29	0.29	2.86	2.86
6-methyl-5-hepten-2-one	n.d.	0.11	0.11	2.44	2.44
citral	n.d.	0.30	0.30	2.87	2.87
glyoxal	1st hydration: 207 ^f 2nd hydration: 20000 ^f	4135.21 ^g	0.02 ^g	1.67	7.01
formaldehyde	2000 ^f	47.17 ^e	0.02	1.77	5.07
acetaldehyde	1.20 ^f	0.14 ^e	0.06	2.20	2.55
propionaldehyde	0.85 ^f	0.11 ^e	0.06	2.19	2.45

^aTesting compound. ^bFrom this study unless otherwise noted. ^cCalculated using eq 7. ^dConverted from H values accordingly. ^eThe average of previously measured data summarized by Sander.⁵ ^fPrevious published data recommended by Tilgner et al.⁷ ^gReported by Ip et al.⁸ n.d.: Not detected due to the absence of the hydrated product peak.

85 To better show the difference in partitioning for target compounds using $H_{s,\text{eff}}^{\text{cp}}$ ($K_{\text{wa,eff}}$)
 86 and H_s^{cp} (K_{wa}), points using H_s^{cp} (K_{wa}) values have been included in Figure S5. The difference
 87 is observable, but it does not affect the overall partitioning significantly.

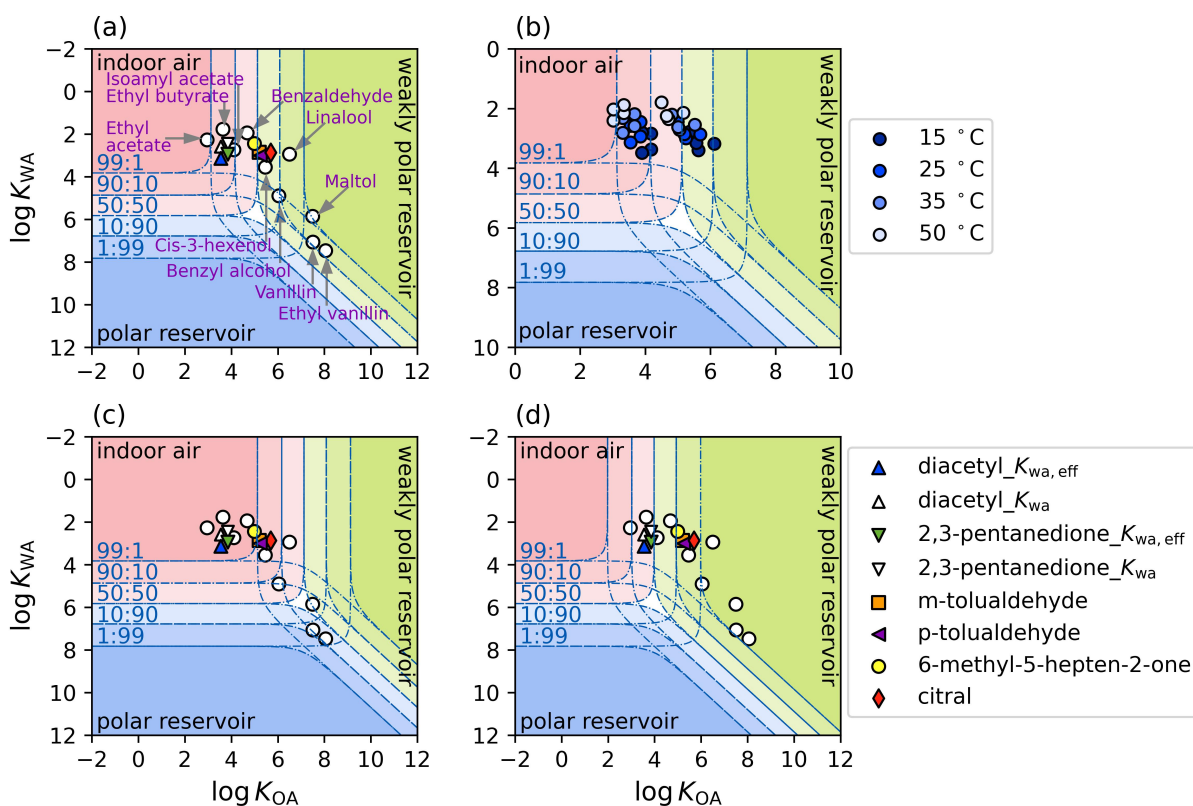


Figure S5: Indoor phase distribution of flavoring agents in e-cigarettes and hookah tobacco. The colored markers are the target compounds in this work, the white dots are the top ten most frequently added flavoring ingredients.⁹ (a) An indoor environment with polar and weakly-polar surface reservoirs equivalent to thicknesses of 500 and 2500 nm under 25 °C. (b) Same assumption as (a) at 15, 25, 35, and 50 °C including target compounds studied in this work; (c) An indoor environment with polar and weakly-polar surface reservoirs equivalent to thicknesses of 500 and 25 nm under 25 °C; (d) An indoor environment with polar and weakly-polar surface reservoirs equivalent to thicknesses of 500 nm and 35 μm under 25 °C.

88 References

- 89 (1) Shunthirasingham, C.; Lei, Y. D.; Wania, F. Evidence of Bias in Air-Water Henry's
 90 Law Constants for Semivolatile Organic Compounds Measured by Inert Gas Stripping.
 91 Environmental Science & Technology **2007**, *41*, 3807–3814.
- 92 (2) Roth, C. M.; Goss, K.-U.; Schwarzenbach, R. P. Adsorption of a diverse set of organic
 93 vapors on the bulk water surface. Journal of Colloid and Interface Science **2002**, *252*,
 94 21–30.

- 95 (3) Shunthirasingham, C.; Cao, X.; Lei, Y. D.; Wania, F. Large bubbles reduce the surface
96 sorption artifact of the inert gas stripping method. Journal of Chemical & Engineering
97 Data **2013**, 58, 792–797.
- 98 (4) Ulrich, N., Endo, S., Brown, T.N., Watanabe, N., Bronner, G., Abraham, M.H., Goss,
99 K.-U., UFZ-LSER database v 3.2 [Internet], Leipzig, Germany, Helmholtz Centre for
100 Environmental Research-UFZ. <http://www.ufz.de/lserd>, 2017; Last access: 2022-08-
101 26.
- 102 (5) Sander, R. Compilation of Henry's law constants (version 4.0) for water as solvent.
103 Atmospheric Chemistry and Physics **2015**, 15, 4399–4981.
- 104 (6) Hilal, S. H.; Ayyampalayam, S. N.; Carreira, L. A. Air- liquid partition coefficient for
105 a diverse set of organic compounds: Henry's law constant in water and hexadecane.
106 Environmental Science & Technology **2008**, 42, 9231–9236.
- 107 (7) Tilgner, A.; Schaefer, T.; Alexander, B.; Barth, M.; Collett Jr, J. L.; Fahey, K. M.;
108 Nenes, A.; Pye, H. O.; Herrmann, H.; McNeill, V. F. Acidity and the multiphase chem-
109 istry of atmospheric aqueous particles and clouds. Atmospheric Chemistry and Physics
110 **2021**, 21, 13483–13536.
- 111 (8) Ip, H. S.; Huang, X. H.; Yu, J. Z. Effective Henry's law constants of glyoxal, glyoxylic
112 acid, and glycolic acid. Geophysical Research Letters **2009**, 36, L01802.
- 113 (9) Omaiye, E. E.; McWhirter, K. J.; Luo, W.; Tierney, P. A.; Pankow, J. F.; Talbot, P.
114 High concentrations of flavor chemicals are present in electronic cigarette refill fluids.
115 Scientific Reports **2019**, 9, 1–9.